$$\frac{U_{C1}}{U_0} = x, \quad \frac{U_{C2}}{U_0} = y, \quad \frac{t}{RC_1} = t, \quad \frac{C_2}{C_1} = a, \quad \frac{R}{R_6} - 1 = b \qquad (1)$$

we obtain the set of equations describing the '2D' oscillator:

$$\frac{dx}{dt} = -x + (k_1 - 1)y$$
$$a\frac{dy}{dt} = -x + (k_1 - 2)y - s(y) \qquad (2)$$

Here $s(y) = \pm 1$, namely $s_{i+1}(y) = s_i[1-2H(s_i y-b)]$, where $H(u)$ is the Heaviside function, that is $H(u < 0) = 0$, $H(u \geq 0) = 1$. The value of s alternates discretely between two quantities, +1 and –1. Thus, the phase space of the system is reduced to the '2D' space consisting of two overlapping plane surfaces, $s = 1$ and $s = -1$.

The output voltages are simply $U_{out1} = yk_1U_0$ and $U_{out2} = -s_ik_2U_0$.

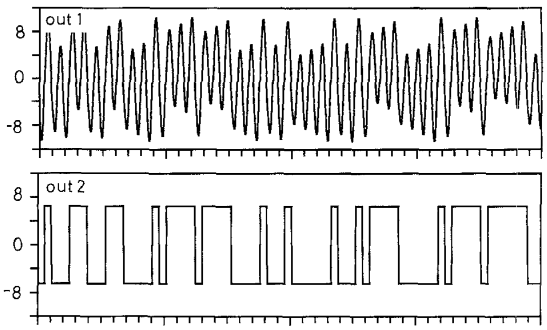

Fig. 3 *Numerical output waveforms at $k_1 = 4.06$, $k_2 = 13$, $a = 2$, $b = 3$, $U_0 = 0.5\,V$*

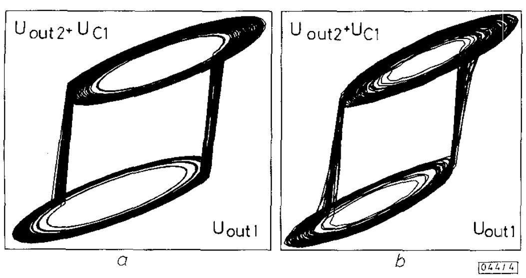

Fig. 4 *Typical phase portraits, ($U_{out2}+U_{C1}$) against U_{out1}*

a Numerical result for parameters given in Fig. 3
b Experimental result for parameters described in *'Experimental results'*

Simulation results: Eqn. 2 has been integrated numerically and the typical results are presented in Figs. 3 and 4*a*.

To characterise the chaotic oscillations quantitatively we have computed the correlation dimension d_{cor} using the algorithm proposed in [11]. The result is $d_{cor} \simeq 2$ for $k_1 = 4.06$, $a = 2$, and $b = 3$ indicating that we deal with a nearly '2D' system.

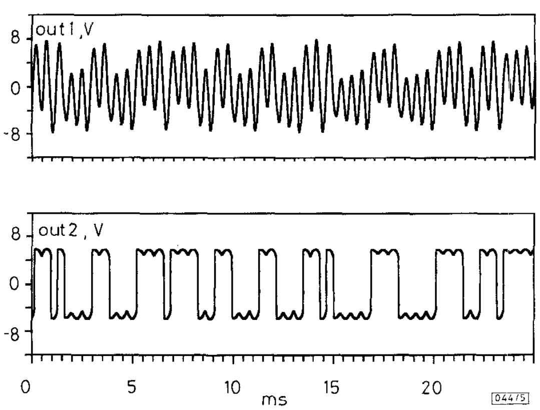

Fig. 5 *Experimental output waveforms U_{out1} and U_{out2} at $k_1 = 4.2$, $k_2 = 13$*

Experimental results: The circuit has been built using the following set of element values: $R_1 = R_2 = 3.9\text{k}\Omega$, $R_3 = 3.6\text{k}\Omega$, $R_4 = 1.2\text{k}\Omega$, $R_5 = R_7 = 12\text{k}\Omega$, $R_6 = 1\text{k}\Omega$, $C_1 = 15\text{nF}$, $C_2 = 33\text{nF}$ with a tolerance of 10%. OA1 and OA2 are LM741 type, or equivalent, operational amplifiers. R4 is an adjustable resistor used to tune the chaotic mode of the oscillations. D1 and D2 are general purpose diodes, e.g. type 1N914 or similar. The output voltages U_{out1}, U_{out2}, and ($U_{out2}+U_{C1}$), have been taken using a digitising oscilloscope TDS 520A. The experimental phase portrait is presented in Fig. 4*b*, and the corresponding waveforms $U_{out1}(t)$ and $U_{out2}(t)$ are shown in Fig. 5.

The oscillations superimposed on the U_{out2} pulses are due to the finite value of R_d, which has been neglected in the equations.

In addition, the correlation dimension of the double-scroll chaotic attractor has been estimated from the experimental time series $U_{out1}(t)$. The obtained experimental quantity $d_{cor} = 2$ is in good agreement with the value computed from the model.

Conclusions: We have designed and examined a simple RC chaotic oscillator exhibiting the double-scroll type chaotic attractor. The circuit can easily be built in any laboratory and can be used for modelling and studying chaotic phenomena.

Acknowledgment: This work was partially supported by the EEC under contract No. ERBCIPDCT940011.

15 April 1996
Electronics Letters Online No: 19960829

A. Tamaševičius, G. Mykolaitis and A. Namajūnas (*Semiconductor Physics Institute, A. Goštauto 11, Vilnius, LT 2600, Lithuania*)

References

1 PIVOVSKY, A.S., and RABINOVICH, M.I.: 'A simple self-sustained oscillator with stochastic behaviour', *Doklady AN SSSR*, 1978, **239**, (2), pp. 301–304 (in Russian, for English translation see *Sov. Phys. Doklady*, 1978, **239**)

2 SHINRIKI, M., YAMAMOTO, M., and MORI, S.: 'Multimode oscillations in a modified van der Pol oscillator containing a positive nonlinear conductance', *Proc. IEEE*, 1981, **69**, (3), pp. 394–395

3 FREIRE, E., FRANQUELO, L.G., and ARACIL, J.: 'Periodicity and chaos in an automomous electronic system', *IEEE Trans. Circuits Syst.*, 1984, **CAS-31**, (3), pp. 237–247

4 MATSUMOTO, T.: 'A chaotic attractor from Chua's circuit', *IEEE Trans. Circuits Syst.*, 1984, **CAS-31**, (12), pp. 1055–1058

5 ZHONG, G.-Q., and AYROM, F.: 'Periodicity and chaos in Chua's circuit', *IEEE Trans. Circuits Syst.*, 1985, **CAS-32**, (5) pp. 501–503

6 MATSUMOTO, T., CHUA, L.O., and KOMURO, M.: 'The double scroll (nonlinear networks)', *IEEE Trans. Circuits Syst.*, 1985, **CAS-32**, (8), pp. 797–818

7 CHUA, L.O., KOMURO, M., and MATSUMOTO, T.: 'The double scroll family: parts I and II', *IEEE Trans. Circuits Syst.*, 1986, **CAS-33**, (11), pp. 1072–1118

8 MORGÜL, Ö.: 'Inductorless realisation of Chua oscillator', *Electron. Lett.*, 1995, **31**, (17), pp. 1403–1404

9 MORGÜL, Ö.: 'Wien bridge based RC chaos generator', *Electron. Lett.*, 1995, **31**, (24), pp. 2058–2059

10 PIKOVSKY, A.S., and RABINOVICH, M.I.: 'Stochastic oscillations in dissipative systems', *Physica D*, 1981, **2D**, (1), pp. 8–24

11 GRASSBERGER, P., and PROCACCIA, I.: 'Characterization of strange attractors', *Phys. Rev. Lett.*, 1983, **50**, (5), pp. 346–349

High-swing cascode MOS current mirror

J. Mulder, A.C. van der Woerd, W.A. Serdijn and A.H.M. van Roermund

Indexing terms: CMOS integrated circuits, Current mirrors

A high-swing cascode triode-region MOS current mirror, basically comprising a triode-region translinear loop, is proposed. A translinear analysis and measurement results are presented.

Introduction: Owing to the trend towards lower supply voltages in modern VLSI systems, many well known conventional circuit techniques are no longer applicable. An important example is the current mirror, a prevalent basic building block. The output voltage swing is severely reduced, especially for high performance implementations, like the cascode and the standard and improved Wilson current mirrors [1].

A number of low voltage high-swing cascode current mirrors have been proposed, e.g. [2, 3]. In these designs, voltage room is gained by operating the grounded MOSTs at the verge of saturation. An even higher output voltage swing is obtained when the grounded MOSTs are operated in the triode region, as was proposed recently in [4].

In this Letter another triode-region high-swing cascode current mirror is presented.

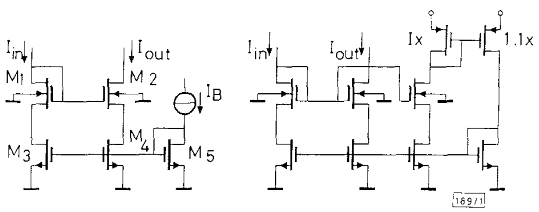

Fig. 1 *Cascode current mirrors using triode-region MOSTs*

Circuit description and measurements: The proposed current mirror is shown in Fig. 1*a*. Transistors M_3 and M_4 are operated in the triode region. The operation of the circuit becomes intuitively clear if we regard M_3 and M_4 as active resistors, biased at a constant gate voltage through the diode-connected transistor M_5. Then, the circuit resembles a simple current mirror, comprising M_1 and M_2, with source degeneration. The degeneration resistors increase the output resistance of the current mirror. As M_4 operates in the triode-region, the mirror provides cascode-type output resistance for output voltages even lower than $2V_{DS,sat}$. The output resistance of the circuit is approximately given by

$$r_{out} \simeq g_{m2} r_{o2} \left(\frac{1}{g_{mD4}} \| r_{o4} \right) \qquad (1)$$

An exact description of the circuit's operation is obtained from a large-signal analysis. A suitable MOST model for the triode region in weak inversion is [5]:

$$I_{DS} = I_o \exp\left(\frac{V_G}{nU_T}\right)\left(\exp\frac{-V_S}{U_T} - \exp\frac{-V_D}{U_T}\right) \qquad (2a)$$

$$= I_f - I_R \qquad (2b)$$

where all symbols have their usual meaning.

Now, a translinear analysis can be performed by recognising that the current mirror basically consists of a translinear loop, comprising two MOSTs operating in the saturation region M_1 and $M2$, and two MOSTs operating in the triode region $M3$ and $M4$. Kirhoff's voltage law yields

$$V_{GS1} - V_{GD3} = V_{GS2} - V_{GD4} \qquad (3)$$

A translinear translation of the KVL in terms of currents is found from eqn. 2*a*: $IDS_1/IR_4 = I_{DS1}/I_{R4}$. I_{DS1} and I_{DS2} equal I_{in} and I_{out}, respectively. The forward currents I_{F3} and I_{F4} both equal $I_{DS5} = I_B$ As the drain currents of M_3 and M_4 equal I_{in} and I_{out}, respectively, their reverse currents are found from eqn. 2*b*: $I_{R3} = I_B - I_{in}$ and $I_B = I_B - I_{out}$. The translinear loop equation thus becomes

$$I_{in}(I_B - I_{out}) = I_{out}(I_B - I_{in}) \qquad (4)$$

The solution of this equation is indeed $I_{out} = I_{in}$.

The deviation from the ideal transfer function of the current mirror shown in Fig. 1*a* was measured using a transistor array. The aspect ratio of the used MOSTs was W/L = 108/7.5µm/µm. The bias current was I_B = 100nA. The results are shown in Fig. 2.

The input current of the current mirror shown in Fig. 1*a* is limited. As I_R is positive by definition, eqn. 4 shows that $I_{in} < I_B$. This limitation can be overcome by using an adaptive biasing method [2, 3], which is illustrated in Fig. 1*b*. By exchanging I_B in eqn. 4 with $A \cdot I_{out}$, where $A > 1$, I_{R3} and I_{R4} remain positive for all values of I_{in}. Correct operation was verified by simulations.

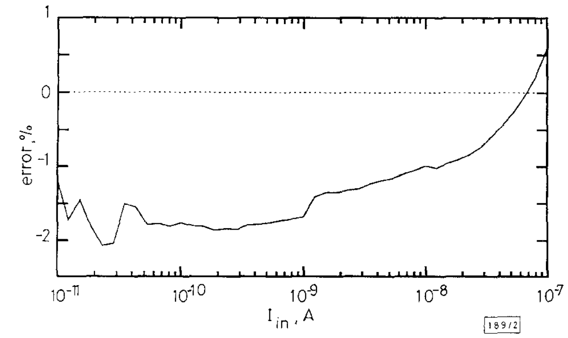

Fig. 2 *Measured error in transfer function*

The operation of the proposed current mirrors is not restricted to the weak inversion region. The circuits only exploit the symmetric property of the triode-region MOST, which is equally valid in the moderate and strong inversion region. Correct operation in the strong inversion region is easily valldated through a strong inversion translinear analysis [6], and was verified by measurements for the circuit shown in Fig. 1*a*.

Conclusions: A novel high-swing cascode triode-region MOS current mirror was presented. The circuit resembles a simple current mirror with source degeneration. As the circuit comprises a triode-region translinear loop, a large signal description was found through a translinear analysis. The operation of the circuit was verified by measurements.

26 April 1996
Electronics Letters Online No: 19960857

J. Mulder, A.C. van der Woerd, W.A. Serdijn and A.H.M. van Roermund (*Electronics Research Laboratory, Delft University of Technology, Mekelweg 4, 2628 CD, Delft, The Netherlands*)

References

1 HART, B.L., and BARKER, R.W.J.: 'D.C. matching errors in the Wilson current source', *Electron. Lett.*, 1976, **12**, (15), pp. 389–390
2 HEIM, P., and JABRI, M.A.: 'MOS cascode-mirror biasing circuit operating at any current level with minimal output saturation voltage', *Electron. Lett.*, 1995, **31**, (9), pp. 690–691
3 BRUUN, E., and SHAH, P.: 'Dynamic range of low-voltage cascode current mirrors'. Proc. ISCAS, 1995, Vol. 2, pp. 1328–1331
4 PRODANOV, V.I., and GREEN, M.M.: 'CMOS current mirrors with reduced input and output voltage requirements', *Electron. Lett.*, 1996, **32**, (2), pp. 104–105
5 ENZ, C.C., KRUMMENACHER, F., and VITTOZ, E.A.: 'An analytical MOS transistor model valid in all regions of operation and dedicated to low-voltage and low-current applications', *Analog Int. Circ. and Signal Process.*, 1995, **8**, (1), pp. 83–114
6 WIEGERINK, R.J.: 'Analysis and synthesis of MOS translinear circuits'. PhD thesis, Twente University of Technology, Enschede, 1992

Data-aided phase tracking detection of Doppler shifted MPSK

L. Bin and P. Ho

Indexing terms: Digital communication systems, Phase shift keying

A new data-aided phase tracking detection for Doppler shifted MPSK is presented, and simulation results are given. It is shown that the data-aided phase tracking detection of Doppler shifted MPSK provides good error performance.

Introduction: In digital communications applications where carrier phase and/or frequency are likely to be uncertain, e.g. a multipath fading enviromnent, noncoherent detection or differential